



Cite this: DOI: 10.1039/d1dt00277e

Reactivity of a T-shaped cobalt(i) pincer-complex†

Regina Matveeva, Clemens K. Blasius, Hubert Wadepohl and Lutz H. Gade *

The reactivity of a paramagnetic T-shaped cobalt(i) complex, $[(iPr)boxmi]Co$, stabilised by a monoanionic bis(oxazolylmethylidene)-isoindolate (boxmi) *NNN* pincer ligand is described. The exposure to carbon monoxide as an additional neutral ligand resulted in the square-planar species $[(iPr)boxmi]Co(CO)$, accompanied by a change in the electronic spin state from $S = 1$ to $S = 0$. In contrast, upon treatment with trimethylphosphine the formation of the distorted tetrahedral complex $[(iPr)boxmi]Co(PMe_3)$ was observed ($S = 1$). Reacting $[(iPr)boxmi]Co$ with iodine (I_2), organic peroxides (tBu_2O_2 , $(SiMe_3)_2O_2$) and diphenyldisulphide (Ph_2S_2) yielded the tetracoordinated complexes $[(iPr)boxmi]Co(I)$, $[(iPr)boxmi]Co(O^tBu)$, $[(iPr)boxmi]Co(OSiMe_3)$ and $[(iPr)boxmi]Co(SPh)$, respectively, demonstrating the capability of the boxmi-supported cobalt(i) complex to homolytically cleave bonds and thus its distinct one-electron reactivity. Furthermore, a square-planar cobalt(ii) alkynyl complex $[(iPr)boxmi]Co(CCAr^F)$ was identified as the main product in the reaction between $[(iPr)boxmi]Co$ and a terminal alkyne, 4-fluoro-1-ethynylbenzene. Putting such species in the context of the previously investigated hydroboration catalysis, its stoichiometric reaction with pinacolborane revealed its potential conversion into a cobalt(ii) hydride complex, thus confirming its original attribution as off-cycle species.

Received 27th January 2021

Accepted 24th March 2021

DOI: 10.1039/d1dt00277e

rsc.li/dalton

Introduction

The reactive potential of low-coordinate low-valent transition metal complexes is well established.^{1–7} Their unsaturated character, both coordinatively and electronically, renders them “activators” of small molecules such as O_2 ,^{8–11} N_2O ,¹² CO_2 ,^{12–14} and N_2 .^{15,16} Moreover, they have also found broad application in a variety of stoichiometric and catalytic group transfer reactions relevant to biological processes.^{17,18}

As part of the research efforts involving earth-abundant 3d metals,^{19–23} the synthesis and exploration of new reaction pathways of monovalent, coordinatively unsaturated cobalt compounds has recently attracted increasing interest.^{24–31} Their kinetic stabilisation is usually provided by bulky multi-dentate ligands. Besides nitrogen donor based spectator ligands such as *nacnac*^{32–35} and bis(imino)pyridine derivatives,³⁶ amidophosphine ligands combining hard and soft ligating units have been found to stabilize electron-rich cobalt(i) complexes.^{37–40}

Pincer ligands have been shown to be very suitable for the stabilization of coordinatively unsaturated cobalt centres.^{41–44} Particular attention has been attributed to T-shaped cobalt(i)

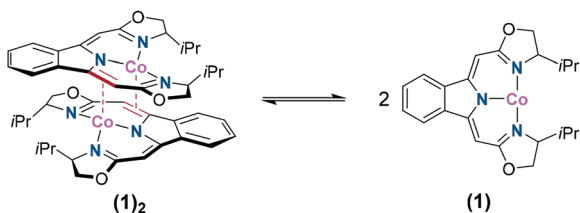
complexes, as they have a readily accessible vacant coordination site, which is essential for the activation of inert chemical bonds. Only few T-shaped cobalt(i) complexes have been reported to date which can be traced back to their reactivity, in particular, their profound tendency to fill the vacant coordination site. The first T-shaped amidophosphine-stabilized cobalt(i) complex was reported by the Caulton group.³⁷ In addition, Fryzuk and co-workers published a phosphine-enamidoiminophosphorane stabilised cobalt(i) complex, which in solution is in equilibrium with the corresponding nitrogen complex and catalyses the conversion of dinitrogen to $N(SiMe_3)_2$.³⁸ Other examples have been reported by our group while attempting to isolate the corresponding PNP cobalt(ii) hydride complex³⁹ as well as Ozerov and coworkers.⁴⁰

We recently synthesized a coordinatively unsaturated *high-spin* cobalt(i) complex (**1**) employing the boxmi^{45,46} ligand family, which is dimeric in the solid-state, $(1)_2$, representing a novel stabilization mode (Scheme 1).⁴⁷ In solution, the dimer was found to be in equilibrium with the T-shaped monomeric species as observed by paramagnetic NMR spectroscopy.

Given the reactive potential of such coordinatively and electronically unsaturated complexes as the boxmi cobalt(i) compound **1**, we recently embarked on a systematic investigation of its reaction patterns. In this first study, the addition of neutral ligands and the resulting coordination geometries and spin states were of interest. In view of its reactivity as a “metallo-radical” single-electron bond cleavage reactions were

Anorganisch-Chemisches Institut, Universität Heidelberg, Im Neuenheimer Feld 270, 69120 Heidelberg, Germany. E-mail: lutz.gade@uni-heidelberg.de

† Electronic supplementary information (ESI) available. CCDC 2056218–2056224. For ESI and crystallographic data in CIF or other electronic format see DOI: 10.1039/d1dt00277e



Scheme 1 The T-shaped cobalt(I) complex [(iPr)boxmi]Co (**1**) in equilibrium with its dimer (**1**)₂ in solution.

of particular interest. Following the observed formation of complex **1** under the conditions of the catalytic hydroboration of terminal alkynes, we also looked into the reactions of an alkynyl species which represents an off-cycle species in the catalytic transformation.

Results and discussion

Addition of neutral donors to the coordinatively unsaturated T-shaped cobalt(I) complex **1**

As starting point for our investigation on the reactivity of boxmi cobalt(I) complex **1**, we examined the propensity of **1** to bind neutral two electron donors. Whereas hard σ -donors such as dialkylethers and trialkylamines were found to be unreactive towards the T-shaped cobalt compound, soft ligands with variable degrees of π -acidity were found to readily coordinate to **1**. The resulting coordination geometry and spin state were primarily determined by the steric demand of the added ligand.

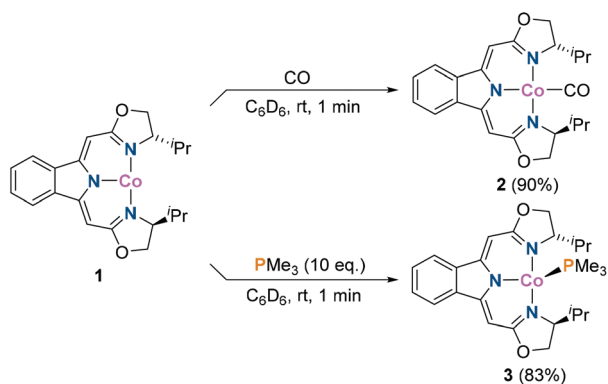
Charging a solution of **1** in C₆D₆ with 5 bar of CO resulted in a rapid change of colour from dark brown to green (Scheme 2, top). The ¹H NMR spectrum revealed the formation of a diamagnetic compound indicating a *d*⁸ low-spin complex, [(iPr)boxmi]Co(CO) (**2**). The infrared spectrum of **2** exhibits one sharp intense vibrational band, which can be assigned to the CO stretching vibration. Compared to similar cobalt(I) mono-

carbonyl complexes based on PCP or PNP ligands ($\nu_{\text{CO}} = 1885\text{--}1899\text{ cm}^{-1}$),^{39,43,48} the stretching frequency of complex **2** with a monoanionic NNN pincer ligand ($\nu_{\text{CO}} = 1918\text{ cm}^{-1}$) and hence the metal π -basicity of the parent cobalt(I) species **1** is slightly lower. The solid-state structure of **2** was determined by X-ray diffraction, with the cobalt centre adopting a square-planar coordination geometry (rms deviation $\leq 0.01\text{ \AA}$, Fig. 1). All structural parameters are within the range expected for such a compound.

The addition of an excess of PMe₃ to a solution of **1** in C₆D₆ was accompanied by a rapid change of colour from dark brown to dark red and yielded complex [(iPr)boxmi]Co(PMe₃) (**3**) in almost quantitative yield (Scheme 2, bottom).

In contrast to the carbonyl analogue, complex [(iPr)boxmi]Co(PMe₃) was found to be paramagnetic. The measurement of the magnetic susceptibility of a C₆D₆ solution of **3** revealed an effective magnetic moment of $2.99\mu_{\text{B}}$, indicating a *high-spin* *S* = 1 ground state. This value is consistent with other previously reported magnetic moments of similar cobalt(I) *high-spin* complexes,^{37,49} the slight deviation from the *spin-only* value (*d*⁸: $\mu_{\text{SO}} = 2.82\mu_{\text{B}}$) being due to the contribution of the orbital angular momentum to the magnetic moment.⁴⁹

The molecular structure of complex **3** in the solid-state was established by X-ray diffraction (Fig. 2). A slightly distorted tetrahedral coordination geometry was found, as reflected in the (N–Co–P) angles of 99.03(4)–103.07(4)°. As indicated above, the difference in the coordination geometry between complexes **1** and **2** can be attributed to a greater steric demand of trimethyl phosphine compared to the carbonyl ligand. The mean P–C bond length (1.8242(2) Å) found for complex **3** is shorter than that in free PMe₃ (1.846(3) Å) while the mean C–P–C angle is larger (102.29(12)° as compared to 98.6(3)°). This indicates a higher *s*-character of the P–C bonds in [(iPr)boxmi]Co(PMe₃) compared to free PMe₃.⁵⁰



Scheme 2 Synthesis of cobalt(I) monocarbonyl and triphenylphosphane complexes **2** (top) and **3** (bottom).

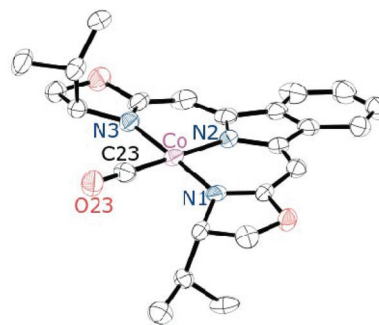


Fig. 1 Molecular structure of monocarbonyl complex [(iPr)boxmi]Co(CO) (**2**) in the solid-state. Hydrogen atoms have been omitted for clarity; displacement ellipsoids are set at 50% probability level; only one of the three independent molecules is shown for **2**. Selected bond lengths [Å] and angles [°] given as range for all independent molecules: Co–N1 1.889(6)–1.903(6), Co–N2 1.935(5)–1.940(6), Co–N3 1.893(6)–1.908(6), Co–C23 1.710(8)–1.724(7), O23–C23 1.155(8)–1.170(9), N1–Co–N2 90.6(2)–91.1(2), N1–Co–N3 177.7(3)–178.7(2), N3–Co–N2 90.4(2)–90.8(2), C23–Co–N2 177.5(4)–178.9(3).

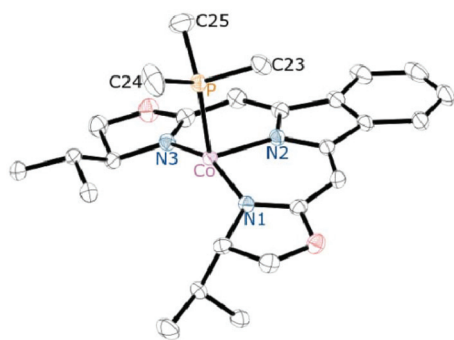


Fig. 2 Molecular structure of trimethylphosphane complex $[(iPr)boxmi]Co(PMe_3)$ (**3**) in the solid-state. Hydrogen atoms have been omitted for clarity; displacement ellipsoids are set at 50% probability level. Selected bond lengths [Å] and angles [°]: Co–P 2.3309(5), Co–N1 1.9349(13), Co–N2 1.9793(14), Co–N3 1.9299(14), P–C23 1.8216(19), P–C24 1.823(2), P–C25 1.828(2), N1–Co–P 100.79(4), N2–Co–P 99.03(4), N3–Co–P 103.07(4), N1–Co–N2 92.26(6), N3–Co–N1 154.25(6), N3–Co–N2 93.43(6), C23–P–C24 101.71(12), C23–P–C25 101.94(10), C24–P–C25 103.22(15).

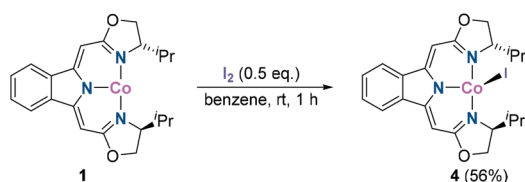
Single-electron bond cleavage reactions

First-row transition metals are generally known for their tendency to favour one-electron over two-electron processes (as *e.g.* associated with oxidative additions).^{39,48} We were therefore interested to probe the potential one-electron redox chemistry associated with homolytic bond cleavage of various substrates (I–I, O–O and S–S).

I–I bond cleavage of iodine. Compound **1** was first reacted with molecular iodine, characterized by its very low I–I bond dissociation energy of 36 kcal mol^{−1},⁵¹ resulting in an immediate change of colour from dark brown to deep red (Scheme 3).

In the ¹H NMR spectrum, a single set of paramagnetic signals was observed which were very broad compared to those previously obtained for the chlorido complex $[(iPr)boxmi]Co(Cl)$.⁵² The high temperature limiting spectrum recorded above 80 °C displayed a signal pattern consistent with *C*₂ symmetry in solution (see ESI†). By means of the Evans method, the magnetic moment of complex **4** in solution was determined to be $\mu_{eff} = 4.27 \mu_B$, consistent with three unpaired electrons and indicating a *high-spin* cobalt(II) *d*⁷ complex. The value is in the range of other known *high-spin* cobalt(II) pincer complexes.^{39,52,53}

For complex $[(iPr)boxmi]Co(I)$, the solid state structure was determined by X-ray diffraction (Fig. 3). The molecular structure confirmed the anticipated four-coordinated cobalt centre coordinated by the boxmi and iodide ligands and showed a



Scheme 3 Synthesis of cobalt(II) iodido complex **4**.

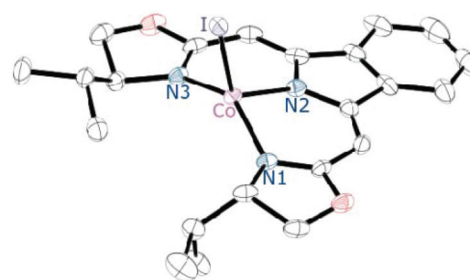


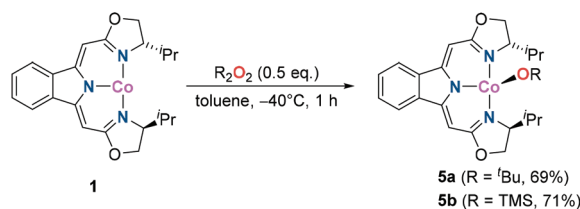
Fig. 3 Molecular structure of iodide complex **4** in the solid state. Hydrogen atoms have been omitted for clarity; displacement ellipsoids are set at 50% probability level; only one of the two independent molecules is shown for **4**. Selected bond lengths [Å] and angles [°], values in square brackets refer to the second independent molecule: Co–I 2.6197(3) [2.5966(3)], Co–N1 1.999(2) [2.000(2)], Co–N2 1.953(2) [1.954(2)], Co–N3 1.997(2) [1.999(2)], N1–Co–I 101.05(6) [104.87(6)], N2–Co–I 120.45(6) [118.25(6)], N3–Co–I 107.98(7) [110.07(6)], N1–Co–N2 92.94(10) [92.74(10)], N3–Co–N1 142.68(10) [137.41(9)], N3–Co–N2 92.13(10) [91.60(9)].

distorted tetrahedral geometry around the cobalt atom. Remarkably, there is a notable difference between the N2–Co–X (X = I, Cl) angles for the respective iodide and chlorido cobalt complexes. In case of $[(iPr)boxmi]Co(I)$, the halide ligand is more strongly tilted towards the isoindolate backbone, as evinced by the N2–Co–X angle of 120.45(6)° (X = I) compared to 127.79° of $[(iPr)boxmi]Co(Cl)$.⁵² This difference can be attributed to the stronger steric demand of iodide compared to the chloride ligand in its repulsive interaction with the isopropyl substituents of the wingtip oxazoline units.

O–O bond cleavage of organic peroxides. Organic peroxides are known to readily undergo (redox-induced) bond cleavage reactions.^{54,55} Therefore, $[(iPr)boxmi]Co$ was next reacted with bis(*tert*-butyl)peroxide (BDE O–O 45.2 kcal mol^{−1})⁵⁶ and bis(trimethylsilyl)peroxide (BDE O–O 54.8 kcal mol^{−1}),⁵⁶ resulting in the corresponding $[(iPr)boxmi]Co(O^tBu)$ (**5a**) and $[(iPr)boxmi]Co(OSiMe_3)$ (**5b**) complexes, respectively (Scheme 4).

Their paramagnetic susceptibilities in solution were determined by the Evans method (**5a**: $\mu_{eff} = 4.05 \mu_B$; **5b**: $\mu_{eff} = 4.11 \mu_B$) and found to be in agreement with the expected values for *d*⁷ *high-spin* complexes.^{39,52,53}

The solid-state structures of both complexes, $[(iPr)boxmi]Co(O^tBu)$ and $[(iPr)boxmi]Co(OSiMe_3)$, were determined by X-ray diffraction (Fig. 4). As for the tetracoordinated iodide complex **4**, distorted tetrahedral coordination geome-



Scheme 4 Synthesis of complexes $[(iPr)boxmi]Co(O^tBu)$ (**5a**) and $[(iPr)boxmi]Co(OSiMe_3)$ (**5b**).

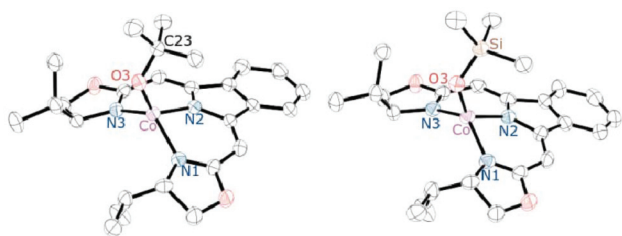


Fig. 4 Molecular structure of complexes **5a** (left) and **5b** (right) in the solid state. Hydrogen atoms have been omitted for clarity; displacement ellipsoids are set at 50% probability level; only one of the two independent molecules is shown for **5a** and **5b**. Selected bond lengths [Å] and angles [°], values in square brackets refer to the second independent molecule, for **5a**: Co–O3 1.855(3) [1.865(3)], Co–N1 2.000(3),[‡] Co–N2 1.989(3) [1.986(4)], Co–N3 2.012(3) [2.016(4)], O3–Co–N1 110.15(12),[‡] O3–Co–N2 128.35(12) [125.25(13)], O3–Co–N3 109.66(12) [107.92(13)], N1–Co–N3 129.18(13) [129.2(4), 140.8(4)], N2–Co–N1 89.4(6) [86.4(4), 93.8(4)], N2–Co–N3 89.81(12) [90.33(16)]; for **5b**: Co–O3 1.867(3) [1.878(4)], Co–N1 1.996(4) [1.993(5)], Co–N2 1.986(4) [1.980(5)], Co–N3 2.001(4) [2.000(5)], O3–Co–N1 107.74(17) [105.33(18)], O3–Co–N2 128.71(17) [124.71(18)], O3–Co–N3 108.40(17) [107.54(17)], N1–Co–N3 132.88(18) [138.60(18)], N2–Co–N1 89.78(19) [90.32(19)], N2–Co–N3 90.52(18) [91.17(19)].[‡] Co–N1/2 distances not meaningful due to equal distance restraints because of apparent disorder of the boxmi ligand.

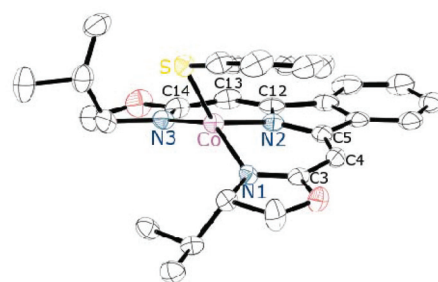


Fig. 5 Molecular structure of thiolate complex **6** in the solid state. Hydrogen atoms have been omitted for clarity; displacement ellipsoids are set at 50% probability level. Selected bond lengths [Å] and angles [°]: Co–S 2.2894(10), Co–N1 2.002(3), Co–N2 1.956(3), Co–N3 2.011(3), N1–Co–S 100.71(8), N2–Co–S 132.40(9), N3–Co–S 105.77(9), N1–Co–N2 91.02(11), N3–Co–N1 140.27(13), N3–Co–N2 92.45(12), C23–S–Co 104.06(11), C12–C13–C14–N3 5.5(5), N1–C3–C4–C5 –1.0(4).

tries around the cobalt atom were observed for **5a** and **5b**. The deformation of the ligand framework is the result of the out-of-plane coordination of the cobalt atom with respect to the plane spanned by the three nitrogen atoms (**5a**: $d = 0.794(2)$ Å;[‡] **5b**: $d = 0.739(3)$ Å [0.657(3) Å]). Based on all metric parameters this deformation was found to be more pronounced for the [(ⁱPr)₃boxmi]Co(O^tBu)] derivative.

S–S-bond cleavage of diphenyl disulphide. Finally, the thiolato complex [(ⁱPr)₃boxmi]Co(SPh)] (**6**) was synthesized by the reaction of [(ⁱPr)₃boxmi]Co] with a stoichiometric amount of Ph₂S₂ (BDE 55 kcal mol⁻¹)⁵⁷ in benzene, accompanied by a rapid change of colour from dark brown to ocre (Scheme 5). The magnetic moment of 4.30 μ_B of complex **6**, as determined by the Evans method, is consistent with a $S = 3/2$ ground state, indicating a *high-spin* cobalt(II) d^7 system.

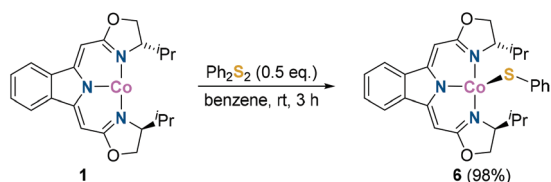
The molecular structure of **6** was established by X-ray diffraction (Fig. 5) and was found to be characterized by a distorted tetrahedral coordination geometry. Notably, the coordination of the SPh fragment leads only to a slight deformation of the boxmi ligand as reflected by torsion angles C12–C13–C14–N3 5.5(5) and N1–C3–C4–C5 –1.0(4)° between the central isoindolato unit and the two flanking oxazoline cycles. The Co–S bond length in **6** is similar to that of a previously reported cobalt(II)

thiolato pincer complex,³⁹ while the N2–Co–S angle of [(ⁱPr)₃boxmi]Co(SPh)] appears to be significantly larger. This difference between the two related complexes can be attributed to the rigidity of the boxmi system compared to the carbazole-based pincer ligand.³⁹

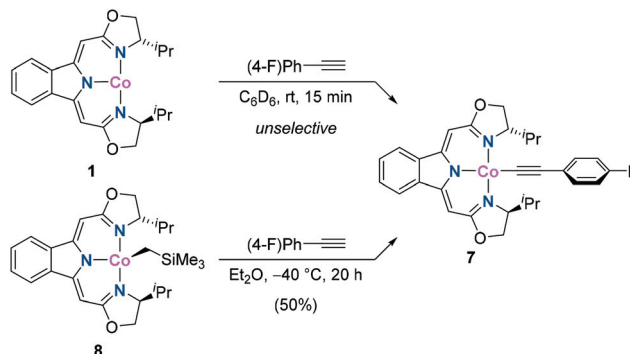
Precatalyst activation pathways in cobalt-catalysed hydroborations of terminal alkynes

In previous studies, we examined the cobalt-catalysed hydroboration of terminal alkynes, selectively furnishing branched alkenyl boronate esters.⁴⁷ As part of the mechanistic investigations, cobalt(I) complex **1** was found as an off-cycle intermediate, which derives from the catalytically active cobalt(II) hydride in the absence of alkynes. Since complex **1** was found to act as a precatalyst for the hydroboration reaction in its own right,⁴⁷ we were interested in further activation pathways.

Treating cobalt(I) complex **1** with stoichiometric amounts of 4-fluoro-1-ethynylbenzene, *i.e.* a terminal alkyne, led to an unselective reaction as apparent from ¹⁹F NMR spectroscopy (Scheme 6, top and ESI† for details). However, cobalt(II) alkynyl complex **7** was isolated as the major component of the reaction mixture (approx. 37% of the resulting material based on NMR) and characterized by X-ray diffraction analysis. Its



Scheme 5 Synthesis of cobalt(II) thiolato complex **6**.



Scheme 6 Synthesis of cobalt(II) alkynyl complex **7**.

independent and selective synthesis was subsequently accomplished by alkane elimination of the cobalt(II) alkyl complex **8** in the reaction with 4-fluoro-1-ethynylbenzene (Scheme 6, bottom).

In contrast to other tetracoordinated Co^{II} complexes in this study, complex [(ⁱPr^{boxmi})Co(CCAr^F)] features a d^7 low-spin ground state ($\mu_{\text{eff}} = 2.39\mu_{\text{B}}$, Evans method). Accordingly, alkynyl complex **7** exhibits an almost perfect (rmsd = 0.017(1) Å) square-planar coordination geometry in the solid-state (Fig. 6), with the boxmi ligand coordinating in the expected meridional fashion and a Co–C23 bond length of $d = 1.899(2)$ Å.

Resulting from the π -accepting properties of the alkynyl ligand, this electronic state is in accordance with a structurally related and previously described alkenyl complex.⁴⁷ As apparent from DFT calculations, the unpaired spin density is efficiently delocalized on the alkynyl ligand, the nitrogen donor atoms and also on the π -system of the boxmi ligand (Fig. 7). In accordance with the comparatively small Fermi contact shifts observed for most of the signals in low-spin complex **7**, the spin density on the ligand framework is mainly located in π -type orbitals. With respect to the metal centre,

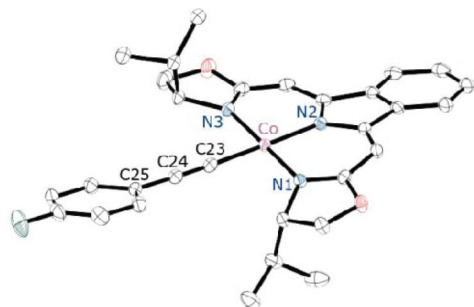


Fig. 6 Molecular structure of complex **7** in the solid state. Hydrogen atoms have been omitted for clarity; displacement ellipsoids are set at 50% probability level. Selected bond lengths [Å] and angles [°]: Co–C23 1.899(2), Co–N1 1.9218(19), Co–N2 1.9487(18), Co–N3 1.9265(19), N2–Co–C23 178.36(8), N1–Co–N3 178.59(8).

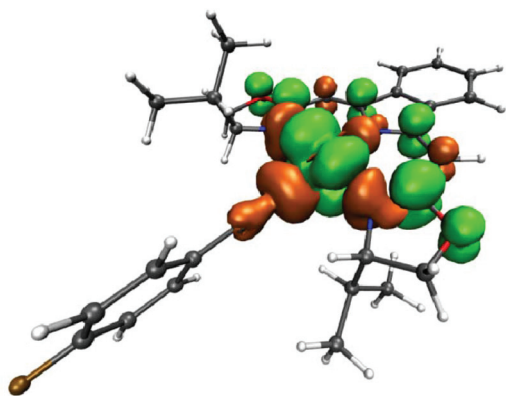
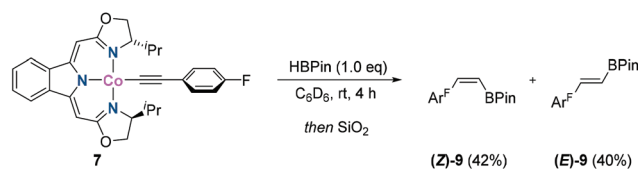


Fig. 7 Visualisation of the spin density distribution in complex **7** (isovalue = 0.0004, positive green, negative orange).



Scheme 7 Role of cobalt(II) alkynyl complex **7** in the hydroboration of terminal alkynes. Relative fractions determined by ¹⁹F NMR spectroscopy. Ar^F denotes a 4-fluorophenyl group and [Co] represents (ⁱPr^{boxmi})Co fragment.

unpaired spin density is predominantly found in the d_{yz} orbital [x = principal molecular axis].

In order to probe the role of alkynyl complex **7** in the cobalt-catalysed hydroboration of terminal alkynes, its stoichiometric reaction with pinacolborane was studied (Scheme 7). Monitoring the reaction *via* ¹⁹F NMR spectroscopy, initially the emergence of one new species was detected, putatively assigned as a cobalt alkenyl complex with a *pro*-(*Z*) configuration (see schematic illustration and ESI† for details).

In the course of the reaction, the gradual conversion of such species into the corresponding *pro*-(*E*)-configured product was observed. The occurrence of such (*E*)-(*Z*)-isomerization of an alkenyl complex has been also described in previous studies.^{47,58} Additionally, this assignment could be confirmed after hydrolytic work-up of the mixture, furnishing the two isomeric linear alkenyl boronate esters as sole products in the expected ratio of approximately 1 : 1 (Scheme 7). Since the formation of product (*Z*)-**9** was not observed under catalytic conditions with precatalyst **8**, complex [(ⁱPr^{boxmi})Co(CCAr^F)] is thought to play an off-cycle role in the hydroboration reaction. However, its conversion into a catalytically active cobalt(II) hydride intermediate *via* a σ -bond metathesis reaction with pinacolborane and thus its re-entry into the main catalytic cycle was found to be feasible.

Conclusion

In this work, we have investigated the coordination behaviour and reducing capability of a coordinatively unsaturated cobalt (I) complex **1** generated in solution from its aggregated dimer. A pronounced dependency of the coordination geometry on the respective neutral two-electron donor ligand (CO *versus* PMe₃) was found for d^8 configured, tetracoordinated cobalt(I) complexes. Furthermore, a strong tendency of the cobalt(I) complex **1** to engage in one-electron redox processes was demonstrated, resulting in various cobalt(II) species. Such behaviour was both observed in homolytic E–E bond cleavage reactions (E = heteroelement) and in the reaction with a terminal alkyne, giving rise to an alkynyl species.

Experimental section

General remarks

All experiments were carried out under an argon atmosphere (Argon 5.0 purchased from Messer Group GmbH and dried over Granusic phosphorus pentoxide granulate prior to use) by means of standard glove box or Schlenk techniques. Solvents were dried by passing through activated alumina columns (M. Braun SPS 800) and stored in glass ampules under argon atmosphere. Deuterated solvents were purchased from Deutero GmbH, dried with potassium (C_6D_6) or sodium ($Tol-d_8$), vacuum distilled, degassed and were stored in glass ampules in a glove box. Cobalt(i) complex **1** and cobalt(ii) alkyl complex **8** were synthesized according to literature procedures.⁴⁷ All other reagents were purchased from commercial suppliers and employed without further purification unless explicitly stated otherwise. All liquids were degassed by three freeze–pump–thaw cycles before use. Iodine was sublimated prior to use. NMR spectra were recorded on a Bruker Avance (200 MHz), a Bruker Avance II (400 MHz) or a Bruker Avance III (600 MHz, equipped with a QNP Cryo Probe) spectrometer. Chemical shifts (δ) are given in parts per million (ppm) relative to tetramethylsilane and are referenced to residual protio solvent signals (1H) or carbon resonances (^{13}C) or to CCl_3F (^{19}F) as external standard.⁵⁹ In order to indicate the signal multiplicities, the following abbreviations were used: singlet (s), doublet (d), triplet (t), multiplet (m). Mass spectra were acquired on JEOL AccuTOF GC time-of-flight (EI) spectrometer at the mass spectrometry facility of the Organic Department at the University of Heidelberg. Elemental analysis measurements were performed on a Vario MICRO Cube elemental analyser at the Microanalysis Laboratory of the Faculty of Chemistry and Earth Sciences at the University of Heidelberg. Magnetic susceptibilities in solution were determined employing the Evans Method according to literature procedures.^{60,61} UV/vis spectra were acquired on a Cary 5000 UV/vis/NIR spectrometer and were baseline and solvent corrected. Single crystal X-ray diffraction experiments were performed on an Agilent SuperNova-E CCD at low temperature with Mo- K_α or Cu- K_α radiation at laboratory for structural analysis of the Institute of Inorganic Chemistry at the University of Heidelberg.

[[^{iPr}boxmiCo(CO)] (2): Compound **[[^{iPr}boxmiCo] (1)** (15.0 mg, 35.4 μ mol, 1.0 eq.) was dissolved in 600 μ L C_6D_6 and exposed to a carbon monoxide atmosphere (5 bar) in a high-pressure tube. Instantaneously, a colour change to dark green was observed. The reaction mixture was filtered and freed from any volatiles *in vacuo*, yielding the product as green solid (14.4 mg, 31.9 μ mol, 90%). Single crystals of **2** suitable for X-ray crystallography were obtained by slow evaporation of a saturated solution in *n*-pentane/diethylether. $C_{23}H_{26}CoN_3O_3$ (451.41) calcd: C 61.20, H: 5.81, N: 9.31; found: C: 60.62, H: 5.36, N: 9.39. 1H NMR (600.13 MHz, $CDCl_3$, 295 K): δ = 7.57–7.55 (m, 2H), 7.13–7.11 (m, 2H), 6.52 (s, 2H), 4.47 (dt, J = 8.5 Hz, J = 2.7 Hz, 2H), 3.91 (dd, J = 8.5 Hz, J = 2.6 Hz, 2H), 3.74 (t, J = 8.5 Hz, 2H), 2.77–2.70 (m, 2H), 0.76 (d, J = 7.0 Hz, 6H), 0.51 (d, J = 7.0 Hz, 6H) ppm. ^{13}C NMR (150.90 MHz,

$CDCl_3$, 295 K): δ 165.1, 156.9, 139.3, 128.3, 120.3, 81.2, 76.6, 66.8, 35.6, 19.0, 14.2. IR (ATR): ν_{CO} = 1918 cm^{-1} .

[[^{iPr}boxmiCo(PMe₃)] (3): Compound **[[^{iPr}boxmiCo] (1)** (20 mg, 47.2 μ mol, 1.0 eq.) was dissolved in 600 μ L benzene and an excess of trimethylphosphine (50 μ L, 35.9 mg, 472 μ mol, 10 eq.) was added. The dark red solution was freed from any volatiles *in vacuo* and washed with *n*-pentane, yielding the product **3** as a red solid (19.6 mg, 39.2 μ mol, 83%). Single crystals of **3** suitable for X-ray crystallography were obtained by slow diffusion of *n*-pentane into a saturated solution of **3** in toluene at -40 °C. $C_{25}H_{35}CoN_3O_2P$ (449.48) calcd: C 60.12, H 7.06, N 8.41; found: C 60.38, H 6.98, N 8.40. 1H NMR (600.13 MHz, C_6D_6 , 295 K): δ = 103.91 (s, 2H), 67.74 (s, 9H), 33.77 (s, 2H), 19.79 (s, 2H), 3.33 (s, 2H), 1.79 (s, 6H), -3.35 (s, 2H), -7.66 (s, 2H), -17.93 (s, 6H), -19.42 (s, 2H) ppm. ^{13}C NMR (150.90 MHz, C_6D_6 , 295 K): δ = 349.5 (s), 235.8 (d, $^1J_{CH}$ = 131.3 Hz), 166.6 (s), 124.1 (d, $^1J_{CH}$ = 156.8 Hz) ppm. μ_{eff} = 2.99 μ_B (C_6D_6 , Evans, 295 K).

[[^{iPr}boxmiCoI] (4): A solution of iodine (5.99 mg, 23.6 μ mol, 0.5 eq.) in benzene (2 mL) was added to a solution of compound **1** (20.0 mg, 47.2 μ mol, 1.0 eq.) in 1.5 mL benzene at ambient temperature. The dark red solution was stirred for 1 h and was freed from any volatiles *in vacuo*. The residue was washed with *n*-pentane to yield **4** as a dark red solid (18.0 mg, 26.6 μ mol, 56%). Single crystals of **4** suitable for X-ray crystallography were obtained by slow diffusion of *n*-pentane into a saturated solution of **4** in toluene at -40 °C. $C_{22}H_{26}CoIN_3O_2$ (550.31) calcd: C 48.02, H 4.76, N 7.64; found: C 47.90, H 4.73, N 7.60. 1H NMR (600.13 MHz, C_6D_6 , 295 K): δ = 174.4, 90.5, 23.0, 14.0, 11.8, -6.5 , -21.4 , -34.0 , -23.9 , -63.7 , -77.9 ppm. ^{13}C NMR (150.90 MHz, C_6D_6 , 295 K): δ = 813.3 (s), 211.0 (d, $^1J_{CH}$ = 153.5 Hz), 193.5 (d, $^1J_{CH}$ = 160.5 Hz), 28.4 (s) ppm. μ_{eff} = 4.27 μ_B ($Tol-d_8$, Evans, 295 K).

[[^{iPr}boxmiCo(O^tBu)] (5a): Complex **1** (20.0 mg, 47.2 μ mol, 1.0 eq.) was dissolved in toluene (1.0 mL) and cooled to -40 °C. Di-*tert*-butyl peroxide (4.37 μ L, 3.45 mg, 23.6 μ mol, 0.5 eq.) was added dropwise. The reaction mixture was allowed to warm up to 0 °C and was stirred for 1 h at ambient temperature. Then, the solvent was removed *in vacuo* and the residue was washed with *n*-pentane to yield **5a** as a dark brown solid (16.1 mg, 32.5 μ mol, 69%). Single crystals of **5a** suitable for X-ray crystallography were obtained as brown needles by slow diffusion of *n*-pentane into a saturated solution of **5a** in toluene at -40 °C. $C_{26}H_{35}CoN_3O_3$ (496.51) calcd: C 62.90, H 7.11, N 8.46; found: C: 62.18, H: 6.97, N: 8.08 (due to the thermal instability of the compound we were unable to obtain more accurate analytical data in this case). 1H NMR (399.89 MHz, $Tol-d_8$, 295 K): δ = 113.7, 64.3, 19.6, 19.3, 16.2, 14.0, 9.6, 8.6, 6.7, 5.3, 5.2, 4.7, 4.4, -4.1 , -12.5 , -14.5 , -21.0 , -51.6 , -56.4 ppm. ^{13}C NMR (150.90 MHz, $Tol-d_8$, 295 K): δ = 830.0 (s), 583.5 (s), 488.8 (br s), 480.5 (br s), 475.6 (br s), 379.1 (s), 342.8 (s), 233.8 (s), 201.9 (d, $^1J_{CH}$ = 157.0 Hz), 192.5 (d, $^1J_{CH}$ = 154.5 Hz), 185.2 (d, $^1J_{CH}$ = 162.8 Hz), 178.9 (d, $^1J_{CH}$ = 162.7 Hz), 174.8 (br s), 150.8 (br s), 82.4 (br s), 8.9 (br s), 2.9 (br s), -23.0 (br s) ppm. μ_{eff} = 4.05 μ_B ($Tol-d_8$, Evans, 295 K).

[ⁱPr^{boxmi}Co(OSiMe₃)] (5b): Bis(trimethylsilyl)peroxide (5.08 μL, 4.21 mg, 23.6 μmol, 0.5 eq.) was added dropwise to a solution of compound **1** (20.0 mg, 47.2 μmol, 1.0 eq.) in benzene (1.5 mL) and stirred for 1 h at ambient temperature. Subsequently, the solvent was removed under reduced pressure and the residue was washed with *n*-pentane to yield **5b** as a dark brown solid (17.2 mg, 33.6 μmol, 71%). Single crystals of **5b** suitable for X-ray crystallography were obtained as brown needles by slow diffusion of *n*-pentane into a saturated solution of **5b** in toluene at −40 °C. C₂₅H₃₅CoN₃O₃Si (512.59) calcd: C: 58.58, H: 6.88, N: 8.20; found: C: 58.64, H: 6.66, N: 7.93. ¹H NMR (600.13 MHz, C₆D₆, 295 K): δ = 113.4, 69.1, 20.5, 16.6, 15.4, 9.8, 4.8, −3.8, −16.2, −18.9, −28.7, −52.1, −57.9 ppm. ¹³C NMR (150.90 MHz, C₆D₆, 295 K): δ = 310.0 (s), 201.4 (d, ¹J_{CH} = 155.0 Hz, ¹J_{CH} = 152.8 Hz), 185.1 (d, ¹J_{CH} = 153.2 Hz), 157.4 (s) ppm. μ_{eff} = 4.11 μ_B (Tol-*d*₈, Evans, 295 K).

[ⁱPr^{boxmi}Co(SPh)] (6): To a stirred solution of compound **1** (20.1 mg, 47.5 μmol, 1.0 eq.) in benzene (1.0 mL) diphenyl disulfide (5.18 mg, 23.7 μmol, 0.5 eq.) was added. The reaction mixture was stirred for 3 h and then freed from any volatiles *in vacuo*. The crude product was washed with *n*-pentane to afford **6** as a brown-red solid (24.9 mg, 46.7 μmol, 98%). Single crystals of **6** suitable for X-ray crystallography were obtained by slow diffusion of *n*-pentane into a saturated solution of **6** in toluene at −40 °C. C₂₈H₃₁CoN₃O₂S (532.57) calcd: C: 63.15, H 5.87, N 7.89; found: C: 63.27, H: 6.24, N: 7.55. ¹H NMR (600.13 MHz, C₆D₆, 295 K): δ = 124.0, 74.6, 21.4, 21.0, 14.0, 11.5, 4.9, −1.7, −5.9, −21.7, −24.1, −28.5, −29.3, −50.5, −64.3, −74.2 ppm. ¹³C NMR (150.90 MHz, C₆D₆, 295 K): δ = 934.5 (s), 313.4 (d, ¹J_{CH} = 160.0 Hz), 201.1 (s), 60.9 (d, ¹J_{CH} = 155.4 Hz), 3.8 (s) ppm. LIFDI-MS found (calcd): *m/z* = 532.1 (532.2) for C₂₈H₃₁CoN₃O₂S⁺. μ_{eff} = 4.30 μ_B (C₆D₆, Evans, 295 K).

[ⁱPr^{boxmi}Co(CCAr^F)] (7): Cobalt(II) alkyl complex **8** (25.0 mg, 49.0 μmol, 1.0 eq.) was dissolved in 2.0 mL diethyl ether and 1-ethynyl-4-fluorobenzene (5.6 μL, 49.0 μmol, 1.0 eq.) was added. The reaction mixture was layered with *n*-pentane (about 8 mL) and stored at −40 °C for 1–2 d, resulting in the formation of dark brown crystals. Subsequently, the supernatant was removed and the residue was washed with *n*-pentane. The product was obtained as dark brown crystalline solid (13.2 mg, 24.3 μmol, 50%). C₃₀H₃₀CoFN₃O₂ (542.52) calcd: C: 66.42, H: 5.57, N: 7.75; found: C: 66.52, H: 5.91, N: 8.08. ¹H NMR (600.13 MHz, C₆D₆, 295 K): δ = 63.76 (s, 2H), 20.71 (s, 2H), 19.58 (s, 2H), 15.23 (s, 2H), 12.33 (s, 2H), 9.07 (s, 2H), 8.57 (s, 2H), 8.47 (s, 2H), 6.39 (s, 6H), 4.34 (s, 6H), −1.04 (s, 2H) ppm. ¹³C NMR (150.90 MHz, C₆D₆, 295 K): δ = 228.2 (d, *J* = 156.7 Hz), 185.1 (s), 166.4 (d, *J* = 244.3 Hz), 162.6 (d, *J* = 159.3 Hz), 141.5 (s), 120.2 (d, *J* = 155.1 Hz), 116.5 (s), 114.7 (dd, *J* = 163.8 Hz, *J* = 19.6 Hz), 101.8 (t, *J* = 145.4 Hz), 84.3 (s), 61.3 (s), 48.4 (s), 39.0–36.5 (m), 30.8–28.5 (m) ppm. ¹⁹F NMR (376.27 MHz, C₆D₆, 295 K): δ = −111.3 ppm. μ_{eff} = 2.39 μ_B (C₆D₆, Evans, 295 K).

Computational studies

All geometry optimizations and calculations were performed at the DFT level of theory using the Gaussian 09 program without

any symmetry restrictions.⁶² The B3LYP exchange–correlation functional^{63–65} combined with Ahlrich's def2-TZVP (for cobalt and nitrogen) and def2-SVP basis set was employed.^{66,67} Frequency calculations at the same level of theory were performed to identify the optimized structures as stationary points.

X-ray diffraction studies

Details of the structure determinations are provided in the ESL† CCDC 2056218 (for **2**), 2056219 (for **3**), 2056220 (for **4**), 2056221 (for **5a**), 2056222 (for **5b**), 2056223 (for **6**), 2056224 (for **7**)† contain the supplementary crystallographic data for this paper.

Conflicts of interest

There are no conflicts to declare.

Acknowledgements

We acknowledge funding by the University of Heidelberg and the Deutsche Forschungsgemeinschaft (DFG-Ga488/9-2) as well as support by the bwHPC initiative and the bwHPC-C5 project.

References

- 1 Y. C. Tsai, *Coord. Chem. Rev.*, 2012, **256**, 722–758.
- 2 W. B. Tolman, *Activation of Small Molecules: Organometallic and Bioinorganic Perspectives*, John Wiley & Sons, 2006.
- 3 L. J. Taylor and D. L. Kays, *Dalton Trans.*, 2019, **48**, 12365–12381.
- 4 P. P. Power, *Chem. Rev.*, 2012, **112**, 3482–3507.
- 5 C. C. Cummins, *Prog. Inorg. Chem.*, 2007, **47**, 685–836.
- 6 D. C. Bradley and M. H. Chisholm, *Acc. Chem. Res.*, 1976, **9**, 273–280.
- 7 P. P. Power, *Comments Inorg. Chem.*, 1989, **8**, 177–202.
- 8 C. A. Rettenmeier, H. Wadepohl and L. H. Gade, *Angew. Chem., Int. Ed.*, 2015, **54**, 4880–4884.
- 9 X. Hu, I. Castro-Rodriguez and K. Meyer, *J. Am. Chem. Soc.*, 2004, **126**, 13464–13473.
- 10 P. Zimmermann and C. Limberg, *J. Am. Chem. Soc.*, 2017, **139**, 4233–4242.
- 11 D. E. DeRoshia, B. Q. Mercado, G. Lukat-Rodgers, K. R. Rodgers and P. L. Holland, *Angew. Chem., Int. Ed.*, 2017, **56**, 3211–3215.
- 12 L. Roy, M. H. Al-Afyouni, D. E. Derosha, B. Mondal, I. M. Dimucci, K. M. Lancaster, J. Shearer, E. Bill, W. W. Brennessel, F. Neese, S. Ye and P. L. Holland, *Chem. Sci.*, 2019, **10**, 918–929.
- 13 D. L. J. Broere, B. Q. Mercado and P. L. Holland, *Angew. Chem., Int. Ed.*, 2018, **57**, 6507–6511.
- 14 C. Yoo and Y. Lee, *Angew. Chem.*, 2017, **129**, 9630–9634.

- 15 C. E. Laplaza and C. C. Cummins, *Science*, 1995, **268**, 861–863.
- 16 A. R. Fout, F. Basuli, H. Fan, J. Tomaszewski, J. C. Huffman, M. H. Baik and D. J. Mindiola, *Angew. Chem., Int. Ed.*, 2006, **45**, 3291–3295.
- 17 P. L. Holland, *Acc. Chem. Res.*, 2008, **41**, 905–914.
- 18 R. H. Holm, P. Kennepohl and E. I. Solomon, *Chem. Rev.*, 1996, **96**, 2239–2314.
- 19 A. Fürstner, *ACS Cent. Sci.*, 2016, **2**, 778–789.
- 20 J. V. Obligacion and P. J. Chirik, *Nat. Rev. Chem.*, 2018, **2**, 15–34.
- 21 A. Mukherjee and D. Milstein, *ACS Catal.*, 2018, **8**, 11435–11469.
- 22 P. Gandeepan and C. H. Cheng, *Acc. Chem. Res.*, 2015, **48**, 1194–1206.
- 23 V. Papa, K. Junge and M. Beller, *Chem. – Eur. J.*, 2019, **25**, 122–143.
- 24 H. Lei, J. C. Fettinger and P. P. Power, *Inorg. Chem.*, 2012, **51**, 1821–1826.
- 25 Z. Mo, J. Xiao, Y. Gao and L. Deng, *J. Am. Chem. Soc.*, 2014, **136**, 17414–17417.
- 26 J. Hicks and C. Jones, *Organometallics*, 2015, **34**, 2118–2121.
- 27 T. Nguyen, W. A. Merrill, C. Ni, H. Lei, J. C. Fettinger, B. D. Ellis, G. J. Long, M. Brynda and P. P. Power, *Angew. Chem., Int. Ed.*, 2008, **47**, 9115–9117.
- 28 S. S. Rozenel, R. Padilla and J. Arnold, *Inorg. Chem.*, 2013, **52**, 11544–11550.
- 29 T. P. Lin and J. C. Peters, *J. Am. Chem. Soc.*, 2013, **135**, 15310–15313.
- 30 C. A. Sanz, C. A. M. Stein and M. D. Fryzuk, *Eur. J. Inorg. Chem.*, 2020, **2020**, 1465–1471.
- 31 C. Jones, C. Schulten, R. P. Rose, A. Stasch, S. Aldridge, W. D. Woodul, K. S. Murray, B. Moubarak, M. Brynda, G. La Macchia and L. Gagliardi, *Angew. Chem., Int. Ed.*, 2009, **48**, 7406–7410.
- 32 K. Ding, W. W. Brennessel and P. L. Holland, *J. Am. Chem. Soc.*, 2009, **131**, 10804–10805.
- 33 K. Ding, T. R. Dugan, W. W. Brennessel, E. Bill and P. L. Holland, *Organometallics*, 2009, **28**, 6650–6656.
- 34 K. Ding, A. W. Pierpont, W. W. Brennessel, G. Lukat-Rodgers, K. R. Rodgers, T. R. Cundari, E. Bill and P. L. Holland, *J. Am. Chem. Soc.*, 2009, **131**, 9471–9472.
- 35 T. R. Dugan, X. Sun, E. V. Rybak-Akimova, O. Olatunji-Ojo, T. R. Cundari and P. L. Holland, *J. Am. Chem. Soc.*, 2011, **133**, 12418–12421.
- 36 A. C. Bowman, C. Milsman, C. C. H. Atienza, E. Lobkovsky, K. Wieghardt and P. J. Chirik, *J. Am. Chem. Soc.*, 2010, **132**, 1676–1684.
- 37 M. Ingleson, H. Fan, M. Pink, J. Tomaszewski and K. G. Caulton, *J. Am. Chem. Soc.*, 2006, **128**, 1804–1805.
- 38 T. Suzuki, K. Fujimoto, Y. Takemoto, Y. Wasada-Tsutsui, T. Ozawa, T. Inomata, M. D. Fryzuk and H. Masuda, *ACS Catal.*, 2018, **8**, 3011–3015.
- 39 L. S. Merz, C. K. Blasius, H. Wadepohl and L. H. Gade, *Inorg. Chem.*, 2019, **58**, 6102–6113.
- 40 B. J. Foley, C. M. Palit, N. Bhuvanesh, J. Zhou and O. V. Ozerov, *Chem. Sci.*, 2020, **11**, 6075–6084.
- 41 J. Sun, L. Luo, Y. Luo and L. Deng, *Angew. Chem., Int. Ed.*, 2017, **56**, 2720–2724.
- 42 K. Tokmic, C. R. Markus, L. Zhu and A. R. Fout, *J. Am. Chem. Soc.*, 2016, **138**, 11907–11913.
- 43 L. M. Guard, T. J. Hebden, D. E. Linn and D. M. Heinekey, *Organometallics*, 2017, **36**, 3104–3109.
- 44 V. M. Krishnan, H. D. Arman and Z. J. Tonzetich, *Dalton Trans.*, 2018, **47**, 1435–1441.
- 45 (a) Q.-H. Deng, H. Wadepohl and L. H. Gade, *Chem. – Eur. J.*, 2011, **17**, 14922–14928; (b) Q.-H. Deng, H. Wadepohl and L. H. Gade, *J. Am. Chem. Soc.*, 2012, **134**, 2946–2949; (c) Q.-H. Deng, H. Wadepohl and L. H. Gade, *J. Am. Chem. Soc.*, 2012, **134**, 10769–10772; (d) Q.-H. Deng, T. Bleith, H. Wadepohl and L. H. Gade, *J. Am. Chem. Soc.*, 2013, **135**, 5356–5359; (e) Q.-H. Deng, C. Rettenmeier, H. Wadepohl and L. H. Gade, *Chem. – Eur. J.*, 2014, **20**, 93–97; (f) T. Bleith, H. Wadepohl and L. H. Gade, *J. Am. Chem. Soc.*, 2015, **137**, 2456–2459; (g) T. Bleith, Q.-H. Deng, H. Wadepohl and L. H. Gade, *Angew. Chem., Int. Ed.*, 2016, **55**, 7852–7856; (h) V. Vasilenko, C. K. Blasius, H. Wadepohl and L. H. Gade, *Angew. Chem., Int. Ed.*, 2017, **56**, 8393–8397; (i) V. Vasilenko, C. K. Blasius and L. H. Gade, *J. Am. Chem. Soc.*, 2018, **140**, 9244–9254; (j) C. K. Blasius, V. Vasilenko and L. H. Gade, *Angew. Chem., Int. Ed.*, 2018, **57**, 10231–10235; (k) V. Vasilenko, C. K. Blasius, H. Wadepohl and L. H. Gade, *Chem. Commun.*, 2020, **56**, 1203–1206; (l) C. K. Blasius, N. F. Heinrich, V. Vasilenko and L. H. Gade, *Angew. Chem., Int. Ed.*, 2020, **59**, 15974–15977.
- 46 Q.-H. Deng, R. L. Melen and L. H. Gade, *Acc. Chem. Res.*, 2014, **47**, 3162–3173.
- 47 C. K. Blasius, V. Vasilenko, R. Matveeva, H. Wadepohl and L. H. Gade, *Angew. Chem., Int. Ed.*, 2020, **59**, 23010–23014.
- 48 M. J. Ingleson, M. Pink and K. G. Caulton, *J. Am. Chem. Soc.*, 2006, **128**, 4248–4249.
- 49 M. J. Ingleson, M. Pink, H. Fan and K. G. Caulton, *Inorg. Chem.*, 2007, **46**, 10321–10334.
- 50 L. S. Bartell and L. O. Brockway, *J. Chem. Phys.*, 1960, **32**, 512–515.
- 51 S. W. Benson, *J. Chem. Educ.*, 1965, **42**, 502.
- 52 C. K. Blasius, H. Wadepohl and L. H. Gade, *Eur. J. Inorg. Chem.*, 2020, **24**, 2335–2342.
- 53 D. C. Sauer, H. Wadepohl and L. H. Gade, *Inorg. Chem.*, 2012, **51**, 12948–12958.
- 54 V. Fábos, G. Koczó, H. Mehdi, L. Boda and I. T. Horváth, *Energy Environ. Sci.*, 2009, **2**, 767–769.
- 55 J. Sanchez and T. N. Myers, Peroxides and peroxide compounds, organic peroxides, in *Kirk-Othmer Encycl. Chem. Technol*, 2000.
- 56 C. M. Estévez, O. Dmitrenko, J. E. Winter and R. D. Bach, *J. Org. Chem.*, 2000, **65**, 8629–8639.
- 57 B. Becker and W. Wojnowski, *Synth. React. Inorg. Met.-Org. Chem.*, 1984, **14**, 537–556.
- 58 J. V. Obligacion, J. M. Neely, A. N. Yazdani, I. Pappas and P. J. Chirik, *J. Am. Chem. Soc.*, 2015, **137**, 5855–5858.

- 59 G. R. Fulmer, A. J. M. Miller, N. H. Sherden, H. E. Gottlieb, A. Nudelman, B. M. Stoltz, J. E. Bercaw and K. I. Goldberg, *Organometallics*, 2010, **29**, 2176–2179.
- 60 D. F. Evans, *J. Chem. Soc.*, 1959, 2003–2005.
- 61 S. K. Sur, *J. Magn. Reson.*, 1989, **82**, 169–173.
- 62 M. J. Frisch, G. W. Trucks, H. B. Schlegel, G. E. Scuseria, M. A. Robb, J. R. Cheeseman, G. Scalmani, V. Barone, B. Mennucci, G. A. Petersson, H. Nakatsuji, M. Caricato, X. Li, H. P. Hratchian, A. F. Izmaylov, J. Bloino, G. Zheng, J. L. Sonnenberg, M. Hada, M. Ehara, K. Toyota, R. Fukuda, J. Hasegawa, M. Ishida, T. Nakajima, Y. Honda, O. Kitao, H. Nakai, T. Vreven, J. A. Montgomery Jr., J. E. Peralta, F. Ogliaro, M. Bearpark, J. J. Heyd, E. Brothers, K. N. Kudin, V. N. Staroverov, R. Kobayashi, J. Normand, K. Raghavachari, A. Rendell, J. C. Burant, S. S. Iyengar, J. Tomasi, M. Cossi, N. Rega, J. M. Millam, M. Klene, J. E. Knox, J. B. Cross, V. Bakken, C. Adamo, J. Jaramillo, R. Gomperts, R. E. Stratmann, O. Yazyev, A. J. Austin, R. Cammi, C. Pomelli, J. W. Ochterski, R. L. Martin, K. Morokuma, V. G. Zakrzewski, G. A. Voth, P. Salvador, J. J. Dannenberg, S. Dapprich, A. D. Daniels, Ö. Farkas, J. B. Foresman, J. V. Ortiz, J. Cioslowski and D. J. Fox, *Gaussian 09, Revis. B.01*, Wallingford CT, 2009.
- 63 C. Lee, W. Yang and R. G. Parr, *Phys. Rev. B: Condens. Matter Mater. Phys.*, 1988, **37**, 785–789.
- 64 A. D. Becke, *J. Chem. Phys.*, 1993, **98**, 1372–1377.
- 65 A. D. Becke, *J. Chem. Phys.*, 1993, **98**, 5648–5652.
- 66 A. Schäfer, H. Horn and R. Ahlrichs, *J. Chem. Phys.*, 1994, **100**, 5829–5835.
- 67 F. Weigend and R. Ahlrichs, *Phys. Chem. Chem. Phys.*, 2005, **7**, 3297–3305.